HYDROLOGICAL PROCESSES
Hydrol. Process. (2014)
Published online in Wiley Online Library
(wileyonlinelibrary.com) DOI: 10.1002/hyp.10139

Predictive equation for longitudinal dispersion coefficient

T. Disley, B. Gharabaghi,* A. A. Mahboubi and E. A. McBean
School of Engineering, University of Guelph, Guelph, Ontario, N1G 2 W1, Canada

Abstract:

Dye tracing field data were collected in small, steep streams in Ontario and used to calculate longitudinal dispersion coefficients for these headwater streams. A predictive equation for longitudinal dispersion coefficient is developed using combined data sets from five steeper head – water streams and 24 milder and larger rivers. The predictive equation relates the longitudinal dispersion coefficient to hydraulic and geometric parameters of the stream and has been developed using multiple regression analysis. The newly developed equation shows impressive accuracy of predictions for longitudinal dispersion coefficient ($R^2 = 0.86$, RMSE = 25, Nash–Sutcliffe coefficient $E_{ns} = 0.86$ and Index of Agreement $D = 0.96$) for both small, steep headwater streams as well as large, mild rivers. The Froude number has been introduced as a third key parameter to capture the effect of slope of the reach – in addition to the aspect ratio and bed material surface roughness – on the longitudinal dispersion coefficient. The pronounced improvement in the accuracy of the prediction is due to the addition of the Froude number to capture the effect of the slope of the reach on longitudinal dispersion coefficient. Copyright © 2014 John Wiley & Sons, Ltd.

KEY WORDS longitudinal dispersion; dye tracing; dispersion coefficient; travel time; contaminant spill; stream

Received 26 October 2012; Accepted 21 December 2013

INTRODUCTION

Chemical spills, with potential detrimental effects on the environment, are of major concern to watershed managers. Collecting data on the number of spills and the sources of spills is the mandate of the Ontario Ministry of the Environment's SAC. Assessing the risk that the contaminant poses to a community downstream of the spill and reacting to that assessment is also the mandate of the SAC. For spills to water, the time of travel and mixing of a contaminant in a stream provides valuable information for spill response units and water resource managers to mitigate the impacts of the spilled contaminants. The solution of the mass-transport equation to predict the water quality and spills-transport fluxes in natural rivers and channels leads to the one-dimensional dispersion equation derived by Taylor (1954). The majority of research into the mixing of contaminants in streams makes reference to Taylor's equation. Comprehensive evaluation of these studies was provided by Seo and Cheong (1998) and Toprak and Cigizoglu (2008). Some of the theoretical and empirical models that have been widely considered include those by Elder (1959), Fisher (1968,1975), McQuivey and Keefer (1974), Liu (1977), Fischer *et al*. (1979), Iwasa and Aya (1991), Seo and Cheong (1998), and Kashefipour and Falconer (2002). Although these models include the same key input variables, their predictions of longitudinal dispersion vary significantly. In this study, an equation is derived for predicting longitudinal dispersion in natural streams and is compared with previous empirical models. The case study watershed for this research project is the CRW in Ontario, which is a 1000 km^2 area of urban and rural landscapes drained by 90 km of the main Credit River and over 1500 km of tributaries (Figure 1). The number of reported spills by subwatershed within the CRW was analysed using geographic information system tools. Because of the large number of spills occurring in Ontario, and in the CRW in particular, concern for severe environmental contamination and community health is warranted.

The main objective of this study is to investigate the travel time and mixing of a dissolved contaminant in small, steep streams where the literature was lacking and to back calculate the longitudinal dispersion coefficient. The dispersion coefficients were used to develop a new empirical equation to predict longitudinal dispersion for a wide range of natural streams. The specific tasks included the use of field investigations (dye tracer travel time studies) at relatively low, medium and high flow conditions at five selected reaches to calculate longitudinal dispersion. Data were collected for published literature from larger, milder slope rivers in the USA (Deng *et al*., 2001; Tayfur and Singh, 2005) and combined with data collected from the field investigations from

*Correspondence to: B. Gharabaghi, School of Engineering, University of Guelph, Guelph, Ontario N1G 2 W1, Canada.
E-mail: bgharaba@uoguelph.ca

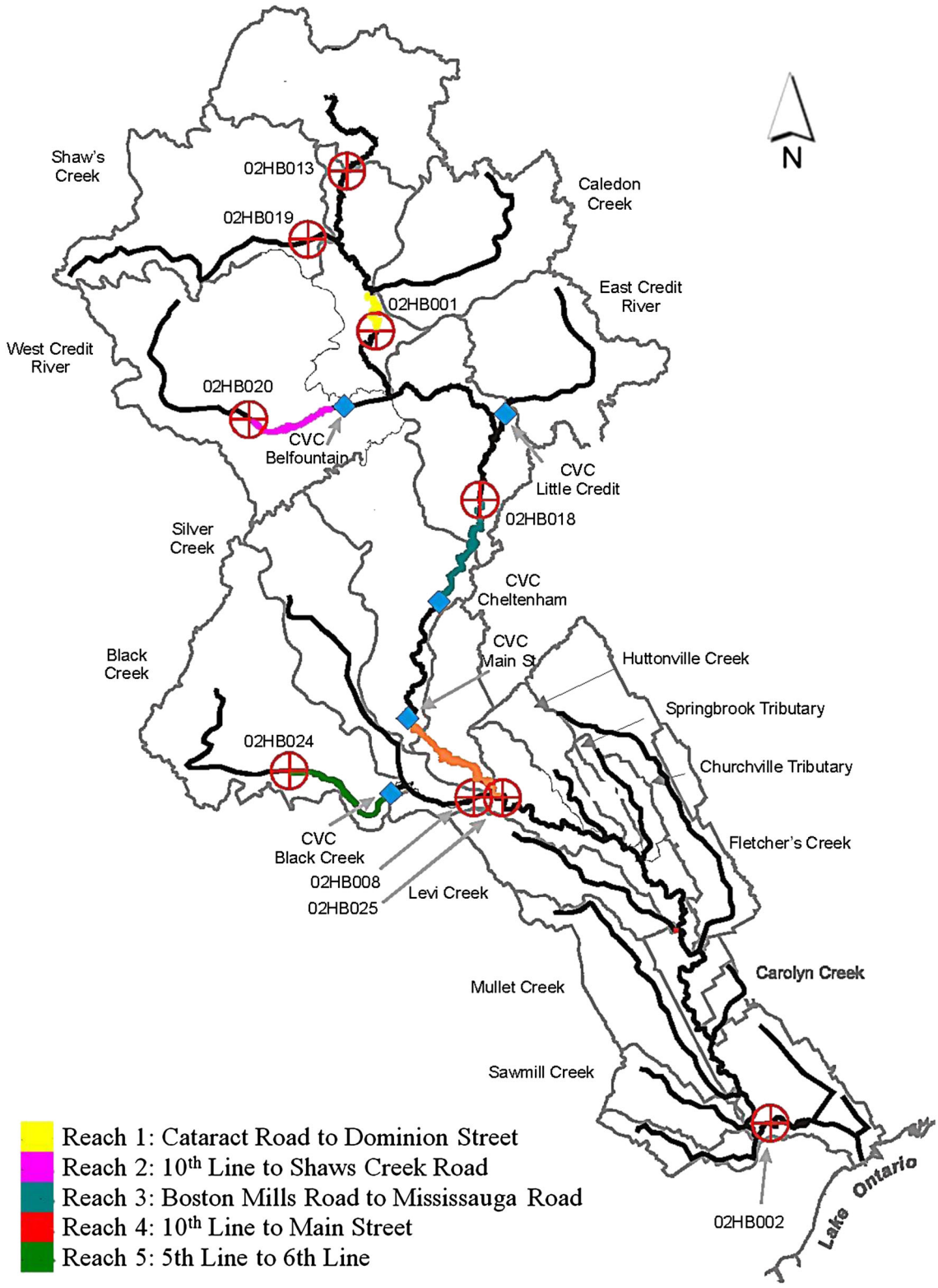

Figure 1. Study reaches in the Credit River watershed, Mississauga, Ontario, Canada. (Source: Base Map Supplied by Credit Valley Conservation Authority, 2004)

small, steep-slope headwater CRW streams (Disley, 2011). The new empirical equation estimates longitudinal dispersion and is applicable to both small, steep streams and large, mild-slope rivers. In addition, previous empirical equations that used to estimate the dispersion coefficient were analysed to assess their

capability in predicting longitudinal dispersion for the expanded data set.

Contaminant transport in surface water

The conservation of mass equation for a constituent is developed by equating the change of mass in a specific volume to the sum of the net advective plus diffusive flux through the volume, plus sources and sinks (Holley and Jirka, 1986). The one-dimensional form of the advective-dispersion equation commonly applied in streams (Yotsukura, 1977) is

$$\frac{\partial C}{\partial t} + \frac{\partial (UC)}{\partial x} = \frac{\partial}{A\partial x}\left(AE\frac{\partial C}{\partial x}\right) - KC \qquad (1)$$

where K is first-order decay rate constant, A (m^2/s) is the cross-sectional area at any location, E (m^2/s) is the longitudinal dispersion coefficient, x (m) is distance, and U (m/s) is average stream velocity. The one-dimensional form of the conservation of mass equation is derived by averaging over one coordinate direction, thus taking and simplifying the two-dimensional form by use of a constant depth in space and time (Maidment, 1992).

Equation (1) has been used to develop a one-dimensional analytical solution for instantaneous slug injections 'with given initial and boundary conditions when the river flow is uniform and the dispersion coefficient is constant' (Seo and Cheong, 1998) and can be applied after the initial mixing period is complete (Chapra, 1997). The analytical solution is

$$C(x,t) = \frac{M}{2\sqrt{\pi E t}} e^{-\frac{(x-Ut)^2}{4Et} - kt} \qquad (2)$$

where C is concentration (μg/l), x is distance downstream of spill (m), t is time (s), M is mass of particles normalized to cross-sectional area (g/m^2), E is longitudinal dispersion coefficient (m^2/s), U is average stream velocity (m/s) and K is first-order decay rate constant.

It is important to note that the *C versus x* distribution is Gaussian for Equation (2) with an instantaneous slug injection; however, the plot of *C versus t* will always exhibit skew (Maidment, 1992). Note that in Equation (2), the only type of diffusive transport process considered is longitudinal dispersion because once the initial mixing period is complete, far enough downstream from the release point, an equilibrium is achieved between transverse mixing and shear, and thereafter, a one-dimensional analysis can be conducted (Maidment, 1992).

In streams and rivers, the size of those found in the CRW, vertical dispersion is the first mixing process to be completed after a slug of dye is injected into the river. Lateral mixing of the dye is completed next, and longitudinal dispersion, having no boundaries, continues indefinitely along the length of the stream. When the one-dimensional advection dispersion model is applied to predict variations of pollutants in natural streams, the selection of a proper dispersion coefficient is the most important and also the most difficult task (Seo and Cheong, 1998).

MATERIALS AND METHODS

Site selection

Five stream locations were chosen for dye tracing in this study (Figure 1).

The injection and sample sites were selected on the basis of their accessibility, depth of water (for the safety of personnel walking in the stream), close proximity to WSC and Credit Valley Conservation Authority (CVC) gauging stations and distance from one another to exceed lateral mixing lengths.

Stream reconnaissance

A stream reconnaissance was completed before any dye tests were to be undertaken to assure the necessary data could be collected to meet the objectives of the study. (1) All injection and sampling sites were inspected for stream accessibility for slug injections and fluorometer, pump and anchor set-up. (2) Stream reaches were inspected using flood line mapping and geographical information systems for dams, outfalls, water intakes and tributaries or any obstructions or obstacles to flow. (3) Discharge measurement points were located on the stream reaches. The WSC and CVC gauging stations were located on the stream reaches for the calculation of load and longitudinal dispersion analysis. (4) The discharge at the sampling site was estimated for selected field days to calculate the amount of dye to be injected at the injection site. The calculation of the amount of dye to be injected is dependent on the type of dye selected. For Rhodamine WT, an empirical equation by Kilpatrick (1970) was used. Kilpatrick's equation allows one to estimate the peak concentration allowing one to optimize fluorometer calibration for increased resolution for Rhodamine WT measurements. (5) Prior to any dye testing, data were collected to calculate and determine the lateral mixing length for various stream reaches. To measure the dye concentration in the middle of the stream, it was necessary to calculate the point downstream from the slug injection where the concentration was fully mixed vertically and laterally in the stream. Hydraulic data were obtained from historical CVC stream velocity measurements to estimate the lateral mixing length. Data were also used from FPMs and DEMs. FPMs and DEMs were used to assess the river system in terms of channel cross-section geometry, stream reach slope, distances, elevation,

manmade obstacles, diversions and accessibility on foot to potential. Once the lateral mixing length was calculated, the injection and sample locations were chosen so that they exceeded the mixing length.

Dye tracing set-up and field procedures

The field procedures were employed to collect time-stamped dye concentrations for dispersion and travel time studies in the CRW. A Turner Designs model 10 AU fluorometer and peristaltic pump were used to pump water from the stream and through the 10 AU fluorometers flow-through cell where measurements of concentration are made and logged to the internal data logger of the 10 AU fluorometer. The field procedures were followed twice at Stream Reach 1 on the same day, one after the other. Both tests resulted in nearly identical time-concentration curves, and it was decided that the field procedures were reproducible. The equipment, set-up and performance of field data collection are described in detail in (Disley, 2011).

RESULTS AND DISCUSSIONS

Load calculation and conservative dye test

The amount of dye recovered in each of the 15 dye tests was calculated using the flow rates available from the closest WSC or CVC gauge station that most accurately represents the flow rate for each stream reach. The gauge stations were chosen so that the least amount of inflow or outflow from the stream exists between the study reaches and gauge station. Where time-concentration curves were incomplete, the last few or first few data points were extrapolated using an exponential fit, as used in previous dye tracer tests to calculate loads by Kratzer and Biagtan (1997). The exponential fit was performed by taking the portion of the dye concentration curve (trailing edge, or leading edge) and exponentially fitting a curve to the data until a concentration of 0.01 ppb is reached. A concentration of 0.01 ppb was chosen because this is the detection limit of the 10 AU fluorometer for Rhodamine WT. It is also noted that dye concentrations utilized in the analysis were not smoothed in any fashion. A conservative tracer is defined as one that displays no losses from the amount injected to the amount measured downstream (Wilson *et al*., 1986). If a tracer is conservative, the total mass injected M_i, upstream will be completely recovered downstream. Jobson (1989) states that the equation to compute the mass of tracer to pass a cross section after complete mixing has occurred is,

$$Mr = \int_{T_e}^{T_f} C\,Q\,dt \tag{3}$$

where M_r is mass recovered, C is concentration, t is time, Q is the discharge in the cross section at time t, T_f is elapsed time to the trailing edge of a dye concentration curve, and T_e is elapsed time of arrival of a time-concentration curve. The equation to calculate the recovery ratio R_r is thus,

$$R_r = \frac{M_r}{M_i} \tag{4}$$

Where M_i is mass injected into the stream. For the conservative dye test, the same injection point and sample point used in the initial dye tests on stream reach #3 were sampled again; however, one additional sample point was added at approximately the halfway point. The dye tests are referred to as 3(A) and 3(B). In an attempt to eliminate any errors in calculating the tracer load, flow measurements were made at sample point 1 (2570 m) with a current velocity metre just before the dye tests. Flow rate was taken from the WSC gauge station for sample point 2 as this flow rate was closest to the sample site and was close to the measured flow rate at sample point 1, which was expected as no inflow or outflow occurred between both points. Table I includes the tracer loads calculated from the original dye tracing tests during relative low, medium and high flow conditions using the flow rates from the nearest WSC gauge station. From the results of these dye tests, and flow measurements, Rhodamine - Rhodamine WT is considered to exhibit a conservative

Table I. Stream reach #3 conservative tracer mass balance

Stream reach #3	Flow rate (m^3/s)	Dye injected (g)	Load measured (g)	Load modelled (g)	Recovery ratio (-)
Sample point #1 (A)	3.91	36	37	35	1.04
Sample point #1 (B)	3.91	36	35	34	0.98
Sample point #2 (A)	3.26	36	40	37	1.13
Sample point #2 (B)	3.26	36	40	36	1.11
Low flow	1.87	36	34	38	0.95
Medium flow	2.38	24	22	23	0.92
High flow	3.63	36	35	35	0.99

nature in the CRW. This phenomenon is somewhat expected when considering, for example, dye tracer experiments by the United States Geological Survey on a 34.27 km sub reach of the Monacacy River in Maryland, USA exhibited approximately 95% recovery rate using Rhodamine WT (Hubbard *et al.*, 1982). More examples of Rhodamine WT recovery rates on streams in the United States were listed in Jobson (1989) and are compiled in Table II.

As can be seen in Tables I and II, the recovery ratios of Rhodamine WT may range around 90–110% in natural streams. Thus, not only are accurate dye concentration measurements critical but also accurate flow rate measurements. Obviously, values greater than 1 are in error, as more dye cannot be measured than injected into the stream. However, as shown in Table I, due to natural variability and the three-dimensional dispersion of the dye – and random errors due to the turbulent nature of flow in the stream – the known total injected mass was not exactly the best-fit back-calculated (i.e. calibrated model parameter) to the simplistic one-dimensional longitudinal dispersion equation (i.e. Equation (2)). Thus, with an appreciation for the possible errors in calculating the mass recovered in dye tracing tests, the recovery ratios obtained in Table II suggest that Rhodamine WT displays a conservative nature in the CRW.

Centroid of time-concentration curve

The movement of a dye cloud passing a cross-sectional location downstream of a spill, or injection, is displayed as a time-concentration curve. Once vertical and lateral mixing is complete, the area under the dye concentration curve remains constant – as the dye travels downstream – for a conservative tracer with no losses (Chapra, 1997). The average travel time from the injection point can be found by calculating the centroid (centre of gravity) of the area under the time-concentration curve using Selby's (1973) trapezoidal approximation method as used in previous dye tracing travel time studies by Kratzer and Biagtan (1997) to find average travel times. The equation used to find the average travel time by the trapezoidal method:

$$\mathrm{Tc} = \frac{\int_0^t C(t)\, t\, dt}{\int_0^t C(t)\, dt} \tag{5}$$

where T_c is elapsed time to the centroid of the time-concentration curve, t is travel time and $C(t)$ is the concentration at time t.

Low, medium and high flow determination

To address the mixing properties of the CRW, dye tests in relatively different flow conditions were performed. To determine if the flow rates could be differentiated as low, medium or high with respect to one another, and with respect to historical flows, the percent of flows that were higher than or exceeded the flow on the day of testing was calculated. The flows were analysed on the basis of the nearest WSC gauge station's historical record of daily average flow rates. The numbers of years used to make the comparison were 84, 26, 27, 21 and 22 for stream reaches 1–5, respectively. Our definition of low, medium and high flow conditions is based on the flow duration analysis as shown in Figure 2. We defined low-flow condition as flows with probability of exceedance less than 80% (representing the low-flow conditions in the summer months), medium flows with the probability of exceedance between 50% and 79% (representing the fall and early winter flow conditions), and high flow conditions for flows with probability of exceedance less than 50% (typical flows during spring freshet).

Longitudinal dispersion calculation

An expression for longitudinal dispersion for two-dimensional channels was produced by Elder (1959), which included a coefficient for the velocity distribution, depth of flow and shear velocity. Fisher (1968) identified

Table II. US streams recovery ratios

River	Length of reach (m)	Flow rate (m^3/s)	Recovery ratio (-)
Shenandoah, Grove Hill	12 700	9.50	1.12
Shenandoah, Grove Hill	24 000	23.20	0.91
Shenandoah, Bixler Bridge	48 100	11.20	0.95
Potomac, Fort Frederick	25 100	17.30	0.91
Potomac, Dam #5	40 700	15.60	1.03
Potomac, Williamsport	9700	19.50	1.08
Cedar C, near Monmouth	3900	3.10	0.90
N Platt, Mystery Bridge	8700	26.60	0.98
N Platte, Cole Cr Rd Br	32 300	26.60	0.92

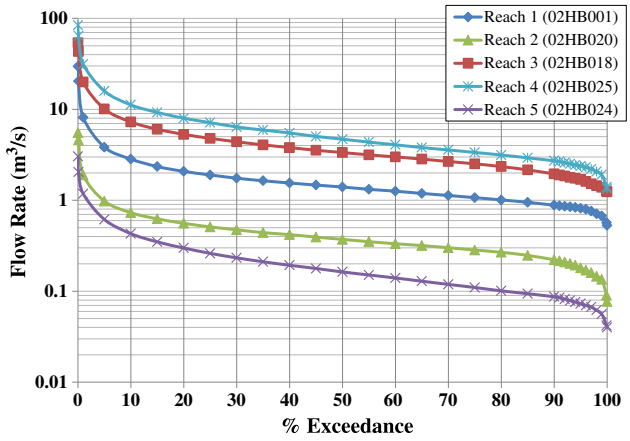

Figure 2. Daily flow duration curves for the study reaches of the Credit River

the lateral velocity distribution as the principal mechanism causing longitudinal dispersion in natural rivers and developed a method following the analytical approach of Taylor and Elder for predicting the dispersion coefficient. Fischer *et al.* (1979) verified his method for predicting dispersion coefficients in natural streams using field data collected by Godfrey and Fredric (1970), which was also used to validate the calculations made for data collected in the CRW.

The quantity of tracer injected, the degree to which the tracer is conservative, the magnitude of the stream discharge and the longitudinal dispersion are factors that must be taken into consideration to predict the concentration of solutes from tracer-concentration data (Jobson, 1989). The first three factors have been accounted for thus far. The longitudinal dispersion factor will now be considered for all 15 dye tests. Once cross-sectional mixing is complete, the process of longitudinal dispersion is the most important mechanism in the mixing of a contaminant in an open body of water (Fisher, 1968). The longitudinal dispersion coefficient is a fundamental parameter in hydraulic modelling of river pollution, for it is a measure of the intensity of the mixing of pollutants in natural streams (Deng *et al.*, 2001).

As all of the dye tests in this study were completed downstream of the complete mixing length, Equation (2) was used to model the time *versus* concentration curves for each dye test and solve for the longitudinal dispersion coefficient E, mass of particles normalized to cross-sectional area M and the average stream reach velocity U. These parameters were solved by choosing the values that minimize the sum of square error between the measured and modelled time-concentration curves for each dye test. The R^2 value represents the field-measured concentration data (including the extrapolated data) compared with the modelled concentrations. All data sets begin and end at 0.01 μg/l, the detection limit of the fluorometer for Rhodamine WT. The calculated dispersion coefficients for the 15 dye tests are listed in Table III.

This method for longitudinal dispersion calculation from raw time-concentration data was tested on time *versus* concentration data collected for CRW study. For instance, this result for medium flow rate of reach study number 1 is depicted in Figure 3, which indicates that the modelled concentration curve fits the measured data very well.

Development of new equation

Selection of significant stream parameters. The key stream parameters that have been found in the literature (Deng *et al.*, 2001; Tayfur and Singh, 2005) to affect the dispersion coefficient, include average stream flow cross-sectional width, depth, longitudinal slope, bed material roughness (friction coefficient) and mean flow velocity. These parameters are summarized in Table IV for a large number of dye tracing tests.

For example, to predict the longitudinal dispersion coefficient, Seo and Cheong (1998) produced the following equation using multiple regression analysis.

Table III. Longitudinal dispersion coefficients for the five study reaches of the Credit River

	Longitudinal dispersion coefficient E (m^2/s)		
Study reach	Low flow	Medium flow	High flow
1	2.35	6.05	5.35
2	2.53	3.02	2.44
3	6.00	7.37	10.20
4	7.13	5.51	8.18
5	1.14	1.91	2.35

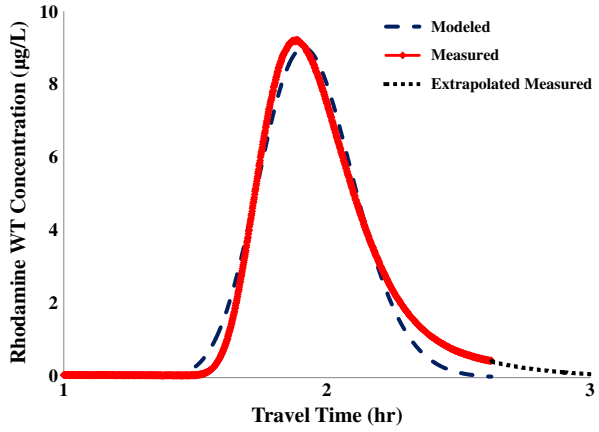

Figure 3. The breakthrough curves for medium flow rate of stream reach 1

Table IV. Credit river watershed hydraulic parameters, USA data and measured dispersion coefficients

Stream	Average width, W (m)	Average depth, d (m)	Average flow velocity, U (m/s)	Average reach slope, s (-)	Shear velocity, u* (m/s)	Dispersion coefficient, E (m^2/s)
Antietam Creek, MD	12.80	0.30	0.42	0.00095	0.57	17.50
	11.89	0.66	0.43	0.00095	0.85	20.90
	21.03	0.48	0.62	0.00100	0.07	25.90
Monocacy River, MD	48.70	0.55	0.36	0.00050	0.05	37.80
	92.96	0.71	0.16	0.00045	0.05	41.40
	51.21	0.65	0.62	0.00040	0.04	29.60
	97.54	1.15	0.32	0.00045	0.58	119.80
Conococheague Creek, MD	42.21	0.69	0.23	0.00060	0.06	40.80
	49.68	0.41	0.15	0.00060	0.08	19.30
	42.98	1.13	0.63	0.00072	0.81	53.30
Chattahoochee River, GA	75.59	2.95	0.74	0.00037	0.14	88.90
	91.90	2.44	0.52	0.00033	0.09	166.90
Difficult Run, VA	14.48	0.31	0.25	0.02720	0.06	1.90
Little Pincy Creek, MD	15.85	0.22	0.39	0.00054	0.05	7.10
Bayou Anacoco, LA	17.33	0.45	0.32	0.00058	0.02	5.80
Tickfau River, LA	14.94	0.59	0.27	0.00061	0.08	10.30
Tangipahoa River, LA	31.39	0.81	0.48	0.00069	0.07	45.10
	161.54	3.96	0.29	0.00009	0.06	130.50
	155.14	1.74	0.47	0.00014	0.04	177.70
Sabine River, LA	116.43	1.65	0.58	0.00013	0.05	131.30
	160.32	2.32	1.06	0.00029	0.05	308.90
Sabine River, TX	14.17	0.50	0.13	0.00018	0.04	12.80
	12.19	0.51	0.23	0.00013	0.03	14.70
	21.34	0.93	0.36	0.00001	0.04	24.20
Wind/Bighorn River, WY	44.20	1.37	0.99	0.00100	0.14	184.60
Copper Creek, VA	16.66	0.49	0.20	0.00085	0.08	16.84
Clich River, VA	48.46	1.16	0.21	0.00332	0.87	14.76
Copper Creek, VA	18.29	0.38	0.15	0.00032	0.12	20.71
Powell River, TN	36.78	0.87	0.13	0.00039	0.05	15.50
Clich River, VA	28.65	0.61	0.35	0.00132	0.07	10.70
Copper Creek, VA	19.61	0.84	0.49	0.00041	0.10	20.82
Clich River, VA	53.24	2.41	0.66	0.00135	0.11	36.93
Copper Creek, VA	16.76	0.47	0.24	0.00020	0.08	24.62
Bayou Anacoco, LA	25.91	0.94	0.34	0.00049	0.07	32.52
	36.58	0.91	0.42	0.00050	0.67	39.48
Nookiack River, WA	64.01	0.76	0.67	0.00096	0.27	34.84
	68.55	2.16	1.55	0.00133	0.17	162.58
John Day River, OR	24.99	0.58	1.01	0.00346	0.14	13.94
	34.14	2.47	0.82	0.00134	0.18	65.03
Yadkin River, NC	70.10	2.35	0.43	0.00044	0.10	111.48
	71.63	3.84	0.76	0.00044	0.13	260.13
Credit River Reach 1: Cataract to Dominion Street (Credit River)	11.21	0.24	0.66	0.01030	0.16	5.35
	10.99	0.21	0.49	0.00911	0.14	6.05
	10.82	0.20	0.41	0.00901	0.13	2.35
Credit River Reach 2: 10th Line to Shaws Creek (West Credit)	5.57	0.31	0.26	0.00296	0.09	2.44
	5.54	0.30	0.15	0.00292	0.09	3.02
	5.10	0.25	0.14	0.00292	0.09	2.53
Credit River Reach 3: Boston Mills to Mississauga Road (Main Credit)	21.64	0.56	0.38	0.00153	0.09	10.20
	20.74	0.48	0.29	0.00152	0.09	7.37
	20.31	0.45	0.26	0.00152	0.08	6.00
Credit River Reach 4: 10th Line to Main Street (Main Credit)	20.97	0.31	0.98	0.00379	0.11	8.18
	19.39	0.26	0.74	0.00340	0.09	5.51
	17.17	0.22	0.52	0.00335	0.09	7.13
Credit River Reach 5: 5th Line to 6th Line (Black Creek)	3.77	0.27	0.23	0.00560	0.12	2.35
	3.57	0.20	0.15	0.00560	0.10	1.90
	3.58	0.19	0.14	0.00560	0.10	1.14

$$\frac{E}{d\,u_*} = 5.195\left(\frac{W}{d}\right)^{0.620}\left(\frac{U}{u_*}\right)^{1.428} \quad (6)$$

where E is longitudinal dispersion coefficient (m^2/s), W is average width of channel (m), d is average depth of channel (m), $\boldsymbol{U}$ is average stream velocity (m/s) and u^* is shear velocity (m/s). Their empirical equation compared better than previous theoretical and empirical equations by Elder (1959), McQuivey and Keefer (1974), Fischer (1975), Liu (1977), and Iwasa and Aya (1991) to a large data set of USA measured longitudinal dispersion coefficients.

However, the water surface slope of each stream reach is also an easily obtainable measurement, which was also available for this data set. McQuivey and Keefer (1974) included the slope of the energy grade line (S) in their longitudinal dispersion coefficient prediction equation. The slope was analysed to determine its relationship with the dimensionless dispersion coefficient. Figure 4 displays a plot of water surface slope *versus* dimensionless dispersion coefficient on Log–Log Scale. The slope *versus* dimensionless dispersion coefficient plot demonstrates that there is a linear trend between the two parameters. When the dimensionless dispersion coefficient increases, slope generally decreases. The direct relationship seen in this graph is likely due to the significant effect that slope has on the shear velocity, or shear stress in the stream, which is also inversely proportional to the longitudinal dispersion coefficient. However, the increase in accuracy of the prediction equation including slope may be the result of another affect slope has on the longitudinal dispersion that relates to lateral turbulence. Miller (1971) concluded that lateral turbulent diffusion coefficient increased with an increase in turbulence intensity when slope increased. If the lateral turbulent diffusion is increased, then it is plausible that the rate of longitudinal dispersion may increase, as

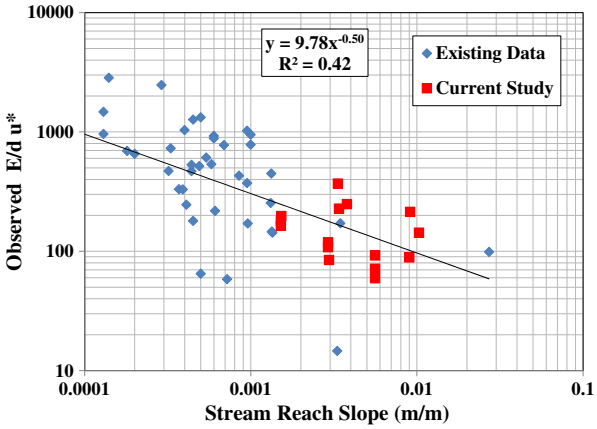

Figure 4. Stream reach slopes *versus* dimensionless longitudinal dispersion coefficient E/d u*

longitudinal dispersion is a function of the velocity variation in the entire cross section also stated by Miller (1971), and Fischer *et al.* (1979). Also of note is that the streams in the CRW in Ontario are different from the streams in the US experiments, as they have larger slopes than the US data set; however, they fall on the same trend line with respect to the dimensionless dispersion coefficient. The average water surface slope for the streams in the CRW is 0.0046, whereas it is 0.0007 for the streams in the US data set.

Statistical analysis. The next step in the development of a prediction equation for longitudinal dispersion was to conduct an ANOVA test on the calculated longitudinal dispersion coefficient for the US data sets, and the 15 data sets in the CRW (Table IV) include the easily obtainable hydraulic and geometric parameters, width (W), mean depth (d), mean velocity (U) and water surface slope (s) for the US data sets and the CRW data sets. The aspect ratio (W/d), friction term (U/u_*) and the stream surface slope (s) were compared using the ANOVA statistical test to determine the effect they have on the measured dispersion coefficient. The details for calculations of the statistical analysis are presented in Table V.

The water surface slopes, width-to-depth ratio and friction term have statistically significant effects on the dimensionless dispersion coefficient. The aspect ratio W/d and the stream bed surface roughness factor U/u_* – inversely proportional to the square root of the Darcy–Weisbach friction factor – are the two key dimensionless characteristics parameters in almost all existing equations presented in Table VI, except for McQuivey and Keefer (1974) that introduced the slope of the reach in their equation. However, in the newly developed Equation (7) in the succeeding texts, we have introduced the Froude number as a third key parameter that reflects the essence of the effect of slope of the reach – in addition to the aspect ratio and bed material surface roughness – on the longitudinal dispersion coefficient as follow:

$$\frac{E}{d\,u_*} = 3.563\left(\frac{U}{\sqrt{g\,d}}\right)^{-0.4117}\left(\frac{W}{d}\right)^{0.6776}\left(\frac{U}{u_*}\right)^{1.0132} \quad (7)$$

Table V. Test of fixed effects to determine the significance on longitudinal dispersion coefficient

Effects	*P* value
Longitudinal slope of the stream reach (s)	3.33E-2
Width to depth ratio of typical stream reach cross section (W/d)	2.77E-04
Stream bed material friction term (U/u_*)	2.49E-08

Table VI. Selected longitudinal dispersion coefficient equations

Investigator	Empirical equation	Reference
McQuivey and Keefer (1974)	$\frac{E}{d\,u_*} = 0.058\left(\frac{1}{s}\right)\left(\frac{U}{u_*}\right)$	Deng *et al.*, 2001
Fischer (1975)	$\frac{E}{d\,u_*} = 0.011\left(\frac{W}{d}\right)^2\left(\frac{U}{u_*}\right)^2$	Riahi-Madvar *et al.*, 2009
Liu (1977)	$\frac{E}{d\,u_*} = 0.18\left(\frac{W}{d}\right)^2\left(\frac{U}{u_*}\right)^{0.5}$	Seo and Cheong (1998)
Koussis and Rodriguez-Mirasol (1988)	$\frac{E}{d\,u_*} = 0.6\left(\frac{W}{d}\right)^2$	Sedighnezhad *et al.* (2007)
Iwasa and Aya (1991)	$\frac{E}{d\,u_*} = 2\left(\frac{W}{d}\right)^{1.5}$	Tavakollizadeh and Kashefipur (2007)
Seo and Cheong (1998)	$\frac{E}{d\,u_*} = 5.195\left(\frac{W}{d}\right)^{0.620}\left(\frac{U}{u_*}\right)^{1.428}$	Seo and Cheong (1998)
Deng *et al.* (2001)	$\frac{E}{d\,u_*} = 0.15\left(\frac{1}{8\,\varepsilon}\right)\left(\frac{W}{d}\right)^{1.667}\left(\frac{U}{U_*}\right)^2$ $\varepsilon = 0.145 + \left(\frac{1}{3520}\right)\left(\frac{W}{d}\right)^{1.38}\left(\frac{U}{u_*}\right)$	Etemad-Shahidi and Taghipour (2012)
Kashefipour and Falconer (2002)	$\frac{E}{d\,u_*} = 10.612\left(\frac{U}{u_*}\right)^2$	Kashefipour and Falconer (2002)
Rajeev and Dutta (2009)	$\frac{E}{d\,u_*} = 2\left(\frac{W}{d}\right)^{0.96}\left(\frac{U}{u_*}\right)^{1.25}$	Azamathulla and Ghani (2010)
This Study	$\frac{E}{d\,u_*} = 3.563\left(\frac{U}{g\,d}\right)^{-0.4117}\left(\frac{W}{d}\right)^{0.6776}\left(\frac{U}{u_*}\right)^{1.0132}$	Equation (7) in this study

All parameters in equations are defined in the notations.

The Froude number $\frac{U}{\sqrt{g\,d}}$ is the ratio of the gravitational forces to inertial forces governing the turbulent motion of the fluid in the stream that mainly depends on the slope of the reach, g is gravitational forces and other parameters are as defined earlier.

In Figure 5, a plot of the calculated dispersion coefficient is plotted against the predicted dispersion coefficient for the same data sets (Table IV) using Equation (7).

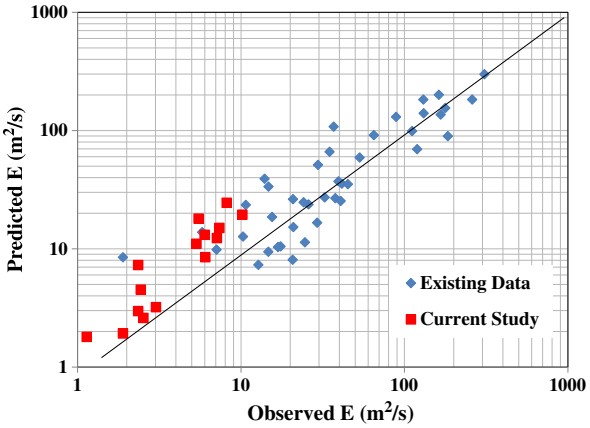

Figure 5. Calculated longitudinal dispersion coefficient E using the new equation developed in this study *versus* measured longitudinal dispersion coefficient

Error analysis. Kashefipour and Falconer (2002) stated that the longitudinal dispersion coefficient E is generally affected by many flow properties and channel geometry parameters and varies within a large range for different sizes and types of channels. Furthermore, large relative error (100%) may occur in predicting the longitudinal dispersion coefficient, especially relatively small values. For these reasons, a statistical analysis based on the measured and predicted values using an logarithm of the predicted and measured values is sensible. On the basis of the methods used by these authors, selected dispersion coefficient equations (summarized in Table VI), were compared. Given that a statistical coefficient may be insufficient and often misleading evaluation criterion, several coefficients were used to assess equation efficiency as depicted in Table VII.

Table VIII shows the values of difference measurements obtained to evaluate the fit between observed and simulated dispersion coefficient. The newly developed model shows impressive accuracy of prediction of the longitudinal dispersion coefficient ($R^2 = 0.86$, RMSE = 25, Nash–Sutcliffe coefficient $E_{ns} = 0.86$ and a very high Index of Agreement $D > 0.96$). The ability of the Seo and Cheong's (1998), Deng *et al.* (2001) and Rajeev and Dutta (2009) equations were found to be similar to our newly developed equation. However, the newly developed equation demonstrated the best predictive longitudinal dispersion coefficient results. The least reliable

Table VII. Statistical coefficients or measures for model evaluation and their range of variability

Coefficient or measure	Equation	Range
Coefficient of determination	$R^2\left[\frac{\sum_{i=1}^{n}(O_i-\overline{O})(P_i-\overline{P})}{\sqrt{\sum_{i=1}^{n}(O_i-\overline{O})^2}\sqrt{\sum_{i=1}^{n}(P_i-\overline{P})^2}}\right]^2$	0–1
Root mean square	$RMS=\sqrt{\frac{\sum_{i=1}^{n}(Pi-Oi)^2}{n}}$	0 to ∞
Coefficient of efficiency Nash and Sutcliffe (1970)	$E_{sn}=1-\frac{\sum_{i=1}^{n}(O_i-P_i)^2}{\sum_{i=1}^{n}(O_i-\overline{O})^2}$	−∞ to 1
Index of agreement Willmott (1982)	$D=1-\frac{\sum_{i=1}^{n}(O_i-P_i)^2}{\sum_{i=1}^{n}(\lvert P_i-\overline{O}\rvert+\lvert O_i-\overline{O}\rvert)^2}$	0–1

Note: n = number of observations, O_i and P_i = observed and predicted values at the time step i, $\overline{O}$ and $\overline{P}$ = mean of observed predicted values at the time step i.

Table VIII. Statistical comparison of dispersion coefficient equations

Dispersion coefficient equations	Statistical methods			
	R^2	RMSE	E_{sn}	D
McQuivey and Keefer (1974)	0.12	276	−16	0.28
Fischer (1975)	0.44	327	−0.23	0.38
Liu (1977)	0.37	108	−1.60	0.65
Koussis and Rodriguez-Mirasol (1988)	0.06	434	−41.21	0.15
Iwasa and Aya (1991)	0.07	165	−5.10	0.33
Seo and Cheong (1998)	0.72	60	0.18	0.87
Deng *et al.* (2001)	0.72	52	0.39	0.89
Kashefipour and Falconer (2002)	0.66	49	0.45	0.88
Rajeev and Dutta (2009)	0.71	55	0.31	0.88
Disley et al. (2013)	0.86	25	0.86	0.96

equations were those of Koussis and Rodriguez-Mirasol (1988) and Iwasa and Aya (1991).

The comparison of estimated dispersion equations with measured data is depicted in Figure 6. This figure shows that the newly developed equation more accurately predicts longitudinal dispersion coefficient with smaller scatter around the 1:1 line. This equation compared favourably with the equations of Seo and Cheong's (1998), Deng *et al.* (2001) and Rajeev and Dutta (2009), with the corresponding correlation coefficient values of 0.86, 0.72, 0.72 and 71, respectively. However, predictions by Koussis and Rodriguez-Mirasol's equation and Iwasa and Aya's equation are found the least reliable relative to those of Liu, Fisher and McQuivey and Keefer's equations as is shown in Figure 7 with larger scatter around the 1 : 1 line.

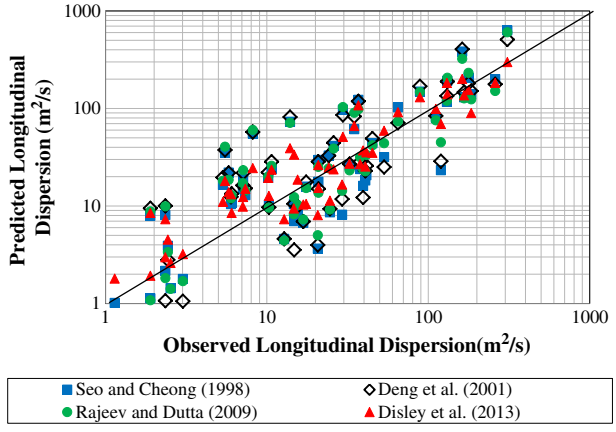

Figure 6. Comparison of predicted dispersion coefficients with measured data for four of the most recent developed equations

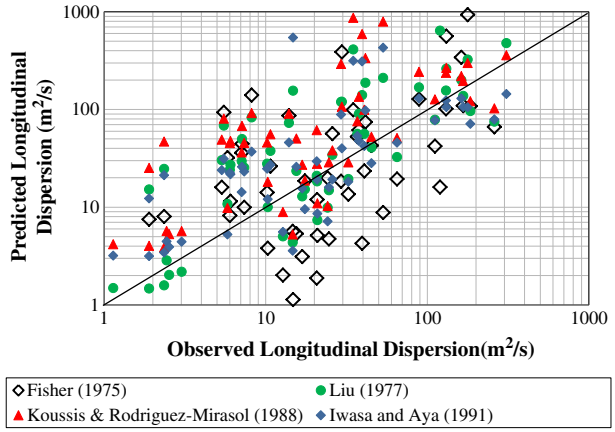

Figure 7. Comparison of predicted dispersion coefficients with measured data for four of the historical well-known equations

Overall, the equation developed in this study compare better than previous theoretical and empirical equations by Rajeev and Dutta (2009), Kashefipour and Falconer (2002), Deng *et al.* (2001), Seo and Cheong (1998), Iwasa and Aya (1991), Koussis and Rodriguez-Mirasol (1988), Liu (1977), Fischer (1975), McQuivey and Keefer (1974) to a large data set of small headwater streams in Ontario (CRW) and USA for measured longitudinal dispersion coefficients.

CONCLUSION

Dye tracing tests were used to characterize longitudinal dispersion coefficients for five small and steep headwater streams of the Credit River, in Mississauga, Ontario, Canada under low, medium and high flow conditions. Longitudinal dispersion coefficients measurements in the literature were previously limited to the vast majority of larger and milder streams. From combined data sets from five steeper headwater streams and 24 milder and larger rivers, a new predictive equation for longitudinal dispersion coefficients is developed. The aspect ratio W/d and the stream bed surface roughness factor U/u_* – inversely proportional to the square root of the Darcy–Weisbach friction factor – are the two key dimensionless characteristics parameters in most existing equations presented in Table VI, except for McQuivey and Keefer (1974) that introduced the slope of the reach in their equation. However, in the newly developed Equation (7) of this study, we have introduced the Froude number as a third key parameter that reflects the essence of the effect of slope of the reach – in addition to the aspect ratio and bed material surface roughness – on the longitudinal dispersion coefficient.

The new predictive equation for longitudinal dispersion coefficient produced accurate estimates both for small headwater streams as well as for larger, milder rivers.

A comparison of this new relationship with the existing equations for the dispersion coefficient using four statistical methods for analysis have shown that the accuracy of this model compared favourably with the equations by Seo and Cheong (1998), Deng *et al.* (2001), Rajeev and Dutta (2009). This increase in predictive capability is due to the addition of the Froude number as a third key parameter that reflects the effect of slope of the reach. The more accurate the estimate of the longitudinal dispersion coefficient so too will be a more accurate estimation of the characteristics of the time-concentration curve.

ANNOTATION

Notation list	Explanation
A	Average cross-sectional area (m^2)
ANOVA (analysis of variance)	Analysis of variance
C	Concentration (μg/l)
CRW	Credit River Watershed
CVC	Credit Valley Conservation Authority
D	Index of Agreement, Willmott (1982)
d	Average depth of channel (m)
DEM	Digital elevation models
E	Longitudinal dispersion coefficient (m^2/s)
E_{ns}	Coefficient of efficiency, Nash and Sutcliffe (1970)
FPM	Flood plain maps
g	Gravitational acceleration (t/s^2)
K	First-order decay coefficient (l/day)
M	Mass of particles normalized to cross-sectional area (g/m^2)
M_i	Mass injected upstream (g)
M_r	Mass recovered downstream (g)
n	Number of observations
O_i	Observed values
$\overline{O}$	Mean of observed values
P_i	Predicted values
$\overline{P}$	Mean of predicted values
Q	Flow rate (m^3/s)
R_r	Recovery ratio (dimensionless)
R^2	Coefficient of correlation
RMS	Root mean square
S	Slope of the energy grade line (dimensionless)
s	Longitudinal slope of the stream reach (m/m)
SAC	Spills Action Centre
t	Time (h)
T_c	Elapsed time to the centroid of the dye cloud (h)
T_e	Elapsed time to the arrival of the leading edge of a dye cloud (h)
T_f	Elapsed time to the trailing edge of the dye cloud (h)
	Average stream velocity (m/s)
u^*	Shear velocity (m/s)
W	Average width of channel (m)
WSC	Water Survey of Canada
x	Distance downstream of a spill (m)

REFERENCES

Azamathulla HM, Ghani AA, Zakaria NA, Aytac G. 2010. Genetic programming to predict bridge pier scour. ASCE. *Journal of Hydraulic Engineering* **136**(3): 165–169.

Chapra S. 1997. Surface water-quality modeling: McGraw-Hill Series in water resource and environmental engineering. *New York: McGraw Hill, Inc. CVC 2010. Water management strategy update*.

Deng ZQ, Bengtsson L, Singh VP, Adrian DD. 2001. Longitudinal dispersion coefficient in single-channel streams. *Journal of Hydraulic Engineering* **128**(10): 901–916.

Disley T. 2011. Travel time modeling assessment for contaminant spills in the credit river watershed. Msc, Dissertation, University of Guelph. pp. 1–154.

Elder JW. 1959. The dispersion of a marked fluid in turbulent shear flow. *Journal of Fluid Mechanics* **5**(4): 544–560.

Etemad-Shahidi A, Taghipour M. 2012. Predicting longitudinal dispersion coefficient in natural streams using M5' Model Tree. *Journal of Hydraulic engineering* **138**(6): 42–554.

Fischer BH. 1975. Discussion of 'simple method for predicting dispersion in streams, by R.S McQuivey and T.N Keefer. *Journal of Environmental Engineering, ASCE* **101**(3): 453–455.

Fischer BH, List EJ, Koh CY, Imberger J, Brooks NH. 1979. *Mixing in Inland and Coastal Waters*. Academic Press, Inc.: New York, N.Y.

Fisher BH. 1968. Dispersion predictions in natural streams. *Journal of Sanitary Engineering Division, ASCE* **994**(SA5): 927–943.

Godfrey R, Fredric kB. 1970. Stream dispersion at selected sites. *U. S. Geological survey professional paper, 433-K, Washington, D.C.*

Holley ER, Jirka GH. 1986. Mixing in rivers, tech.rept. *E-86-11, Corp of engineers, waterways experiment station, Vicksburg, Miss*.

Hubbard EF, Kilpatrick FA, Martens LA, Wilson JF. 1982. Measurement of travel time and dispersion in streams by dye tracing: chapter A9. *Techniques of water-resources investigations of the U.S. Geological survey*, 1–47.

Iwasa Y, Aya S. 1991. Predicting longitudinal dispersion coefficient in open channel flows. Proceedings of international symposium on environ. *Hydraulic., Hong Kong*, 505–510.

Jobson H. 1989. Prediction of travel time and longitudinal dispersion in rivers and streams USGS. Water-resources investigations report. 96–4013.

Kashefipour SM, Falconer RA. 2002. Longitudinal dispersion coefficients in natural channels. *Water Research* **36**: 1596–1608.

Kilpatrick FA. 1970. Dosage requirements for slug injections of Rhodamine BA and WT DYES. *U.S. Geological survey, prof. pater 700-B*, B250–253.

Kratzer CR, Biagtan RN. 1997. Determination of travel times in the lower San Joaquin River Basin, California, from dye-tracer studies during 1994–1995.

Koussis AD, Rodriguez-Mirasol J. 1998. Hydraulic estimation of dispersion coefficient for streams Journal of Hydraulic Engineering, *ASCE* **124**: 317–320.

Liu H. 1977. Predicting dispersion coefficient of streams. *Journal of Environment Engineering Division* **103**(1): 59–69.

Maidment DR. 1992. *Handbook of Hydrology*. McGraw-Hill, Inc.: Washington, D.C.

McQuivey RS, Keefer TN. 1974. Simple method for predicting dispersion in streams. *Journal of Environmental Engineering Division ASCE* **100**(4): 997–1011.

Miller AC. 1971. Turbulent diffusion and longitudinal dispersion measurements in a hydronamically rough open channel flow. PhD dissertation, Colorado State University. Fort Collins, Colorado.

Rajeev RS, Dutta S. 2009. Prediction of longitudinal dispersion coefficients in natural rivers using genetic algorithm. *Hydrology Research* **40**(6): 544–552.

Nash JE, Sutcliffe JV. 1970. River flow forecasting through conceptual models part I–A discussion of principles. *Journal of Hydrology* **10**(3): 282–290.

Riahi-Madvar H, Ayyoubzadeh SA, Khadangi E, Ebadzadeh MM. 2009. An expert system for predicting longitudinal dispersion coefficient in natural streams by using ANFIS. *Expert Systems with Applications: An International Journal* **36**(4): 8589–8596.

Sedighnezhad H, Salehi H, Mohein D. 2007. Comparison of different transport and dispersion of sediments in mard intake by FASTER model. *Proceedings of the Seventh International Symposium River Engineering*, 16–18 October, Ahwaz, Iran, 45–54.

Selby SM. 1973. *CRC Standard Mathematical Tables*, 21st edn. CRC Press: Cleveland, Ohio; 714.

Seo IW, Cheong TS. 1998. Predicting longitudinal dispersion coefficient in natural streams. *Journal of Hydraulic Engineering* **124**(1): 25–32.

Tavakollizadeh A, Kashefipur SM. 2007. Effects of dispersion coefficient on quality modeling of surface waters. *Proceedings of the Sixth International Symposium River Engineering, 16–18 October, Ahwaz, Iran*, 67–78.

Tayfur G, Singh VP. 2005. Predicting longitudinal dispersion coefficient in natural streams by artificial neural network. *Journal of Hydraulic Engineering* **131**(11): 991–1000.

Taylor GI. 1954. Dispersion of matter in turbulent flow through a pipe. *Proc., Royal Soc., London, U.K., Ser. A, 223*, 446–468.

Toprak ZF, Cigizoglu HK. 2008. Predicting longitudinal dispersion coefficient in natural streams by artificial intelligence methods. *Hydrological Processes* **22**(20): 4106–4129.

Willmott CJ. 1982. Some comments on the evaluation of model performance. *Bulletin American Meteorological Society* **63**(11): 1309–1313.

Wilson FF, Cobbjr ED, Kilpatrick FA. 1986. Fluorometric procedure for dye tracing: techniques for water resources investigations of the United States geological survey, Book 3. *Application of Hydraulics, Chapter A12: VIII, U.S. Government printing office, Washington, D.C.*

Yotsukura N. 1977. Derivation of solute-transport equations for turbulent natural-channel flow. *Journal of Research, U.S. Geological Survey* **5**(3): 277–284.